Effects of linear and nonlinear structural deflections on the performance and stability derivatives of high-aspect ratio wing aircraft

Martin Sohst

martin.sohst@tecnico.ulisboa.pt

Instituto Superior Técnico, Universidade de Lisboa, Portugal

November 2017

Abstract

This thesis investigates the influence of linear and nonlinear deflections in a preliminary designed high aspect ratio wing on the performance and stability. For that purpose, first the wing deformations and the flutter speed were calculated with a multidisciplinary design optimization tool and compared. The flutter speed was also compared with a rigid model. To examine a possible mass reduction, a parametric study took place and the results in terms flutter speed are compared with the initial design. Likewise, a longitudinal static stability derivative, C_{m_α}, was estimated with the methods of CFD for the flexible and the rigid wings for characterizing the static stability behaviour.

Keywords: High aspect ratio wing, Aeroelasticity, Flutter, Static stability derivatives, CFD,

1. Introduction

The demand for “greener”, more environmental friendly aircraft increased over the last decades. A reduction of fuel consumption is required as well as lower noise emissions. With the introduction of the latest aircraft and their high level of technology, a peak of improvement was reached for the conventional design. Regarding this, new types of frameworks and radical changes came into the scope of developers. Those include ideas of blended wing bodies, joined wing designs or x-wings as well as strut braced wings or high aspect ratio wings [1]. The latter offers some remarkable improvements: it reduces the lift induced drag, leading to a higher lift over drag ratio; with the same wing area and a higher wingspan, the chord length is reduced, which shortens possible separation lengths. Despite the mentioned benefits, high aspect ratio wings have inherent structural design issues: higher stress levels at the wing root; and higher structural flexibility. With the latter one, the wing is more prone to deflections, that may change the aeroelastic behaviour. Hence, aeroelastic instabilities could occur at lower velocities. Also, with the higher displacements, nonlinear effects tend to occur, changing the behaviour additionally. Those nonlinear effects could be of different origin: geometric, where displacements induce an effective wing span shortage; damping responses, where forces contribute to nonlinear responses; material behaviour, where the stress-strain relation exceeds linear zones.

In this work, the structural deflections of a wing were calculated using an aeroelastic tool based on an equivalent beam model for the structure and potential flow for the aerodynamic model. The linear and nonlinear deformations were compared between each other. The flutter boundary of the deformed wings as well as the rigid wing was estimated for different flight conditions and the results were discussed. A parametric study was devised to assess the influence of further increasing structural flexibility by

decreasing the wing box thickness. To evaluate the stability in a first approach, a static stability derivative of the three models was estimated (C_{m_α}) and the results were assessed.

2. Aeroelasticity and stability

Aeroelasticity

For aeroelasticity a distinction between static and dynamic phenomena is done. The former ones describe the interaction between aerodynamic and elastic forces and their mutual influence. Those are, for instance, *divergence* and *control reversal*. In dynamic behaviour, the inertia forces are also considered in the interaction with aerodynamic and elastic forces. Examples are *buffeting* and *flutter* [2]. In general, an aeroelastic problem can be expressed by:

$$[M]\{\ddot{x}\} + [C]\{\dot{x}\} + [K]\{x\} = \{F\}, \tag{2-1}$$

where $[M]$ is the mass matrix, $[C]$ the structure damping matrix, $[K]$ the structure stiffness matrix, $\{x\}$ the systems DOFs with its time derivatives and $\{F\}$ the load vector. This vector consists of all resulting forces:

$$\{F\} = [M]\{g\} + [A_K]\{x\} + [A_C]\{\dot{x}\}, \tag{2-2}$$

with the gravity vector $\{g\}$, the aerodynamic stiffness matrix $[A_K]$ and the aerodynamic damping matrix $[A_C]$.

Flutter is one of the most critical issues to be handled in aircraft development and its occurrence inevitably leads to a structural failure. Caused on bodies with high aerodynamic loads, for instance wings, tail and control surfaces, it extracts energy from the surrounding airflow, leading to self-excited oscillations [2], as pictured in Figure 2-1:

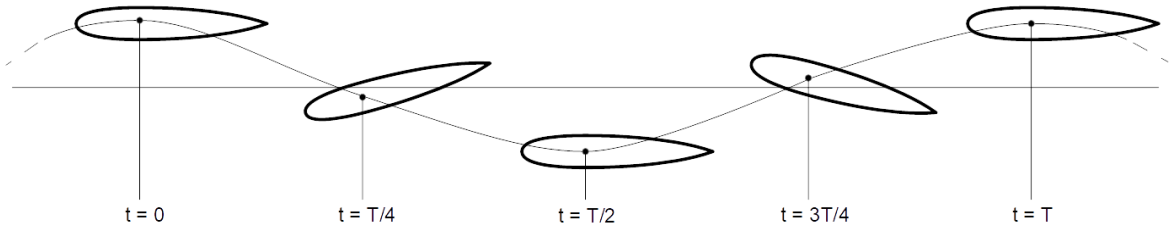

Figure 2-1: Flutter as self-reinforcing oscillation effect of aerodynamic instability

Above a specific speed U_F, the response to a disturbance, like a gust or a high-g manoeuvre, cannot be damped anymore and the structure exhibits a sustained harmonic oscillation. This flutter boundary is marked by the coupling of two rigid body modes. The investigation of flutter within a system is done by studying the stability of infinitesimal motions. In this work, MSC Nastran is used for the analysis with the well-developed p-k-method.

Stability

For the characterization of flight stability, the use of stability derivatives has a broad scope of application [3]. The traditional methods are wind tunnel testing or flight testing with full scale models, but they deal especially with the drawback of high costs [4]. With improved CFD methods, a less cost intensive solution is available.

The stability derivatives can be obtained by a Taylor series expansion [5]. For instance, the pitch moment coefficient C_m can be determined by the expression:

$$C_m = C_{m_0} + C_{m_\alpha}\Delta\alpha + C_{m_{\dot{\alpha}}}\Delta\dot{\alpha} + C_{m_q}q + C_{m_{\dot{q}}}\dot{q} + \hat{\Delta}(\Delta\alpha, q). \tag{2-3}$$

The stability derivatives in the formulation above are the partial derivatives. For the steady solution in an inertial coordinate frame, the time-based terms $(\Delta\dot{\alpha}, \dot{q})$ and the rotational derivative q can be neglected as well as the last term. The static stability derivative C_{m_α} can therefore be estimated by a steady state solution with:

$$C_{m_\alpha} = \frac{\Delta C_m}{\Delta\alpha}, \tag{2-4}$$

meaning it is the slope of the pitching moment coefficient in two time-invariant simulations. Other possibilities for estimation are with finite differences, adjoint methods or automatic differentiation [6].

3. Computational tools and background

For the deformation analysis, a Multidisciplinary Design Optimization tool (MDOGUI) was used [7]. It is based on potential flow equations and valid for incompressible, non-rotational, inviscid flows. With the implemented Prandtl-Glauert correction, an applied corrected pressure coefficient, it is useable for higher subsonic flows with low viscous effects. The aeroelastic model consists of an equivalent beam model for the structural model and a panel model for the aerodynamic model. A fluid-structure-interaction (FSI) model is used to interchange the aerodynamic forces to the structural model and the structural displacements to the aerodynamic model.

The data for modelling the wing in the MDOGUI was extracted from Nastran files provided by an external source. This included structural nodes, material properties, geometrical properties and mass. As only the structural model was available (see Figure 3-1a), airfoil data was taken from a former, comparable project. Some manual design was done regarding the transition from wingtip to winglet to match the structure. To reduce the computational costs for the deformation and flutter calculations, the model was simplified to a lifting surface only (wing). A model of an exemplary calculation is presented in Figure 3-1b.

The calculation of the flutter speed was executed with the commercial program MSC Nastran. The aeroelastic calculations are based on the Doublet Lattice Method (DLM) and the flutter speed estimation uses the p-k-method. The required file for the execution was built with a MATLAB script, using the deformation data of the MDOGUI calculation.

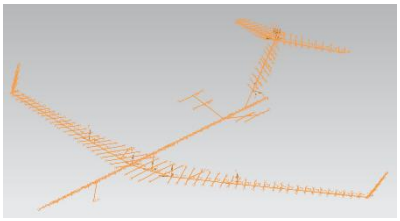

a) Nastran Stick model of the aircraft

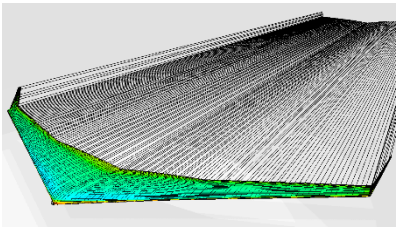

b) Built MDOGUI aeroelastic model

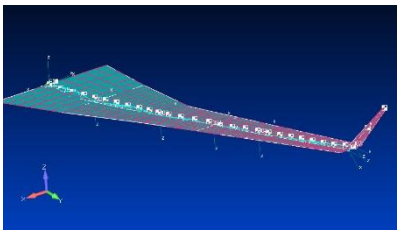

c) Created aeroelastic Nastran model with the MDOGUI data

Figure 3-1: The models used in this work with the provided Nastran stick model (a), the MDOGUI wing model (b) and the created Nastran aeroelastic model (c).

4. Results and discussion

Ahead of results presentation, it should be made clear which arrangement is used for the result discussion, as the used tools differ in their coordinate systems. In Figure 4-1 the coordinate system relative to a wing section is presented, with the x-axis in opposing air flow direction, the y-axis along the wing span and the z-axis in upward (lift) direction. Note furthermore that the structural damping is set to null.

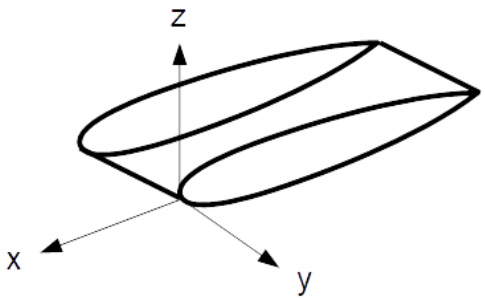

Figure 4-1: Coordinate system specification for the result presentation

4.1. Validation

To validate the model used for the flutter analysis, a comparison between the original stick model and the Nastran model served by MDOGUI data was done. For this purpose, the eigenfrequencies and single loads were taken. For the latter, two point loads, in x-axis and z-axis direction, a moment load around the y-axis and a gravity load were used. The results were close for the eigenfrequencies (below 0.1% for the first 7 modes and below 0.5% for the first 10 modes) as well as for the vertical and gravity loads (both below 0.2%). A higher difference was obtained for the displacement due to the horizontal load and twist, with around 7.5% and 5% respectively. But as the variation is still within 10% and the comparison took place among themselves, it was not seen as problematic.

4.2. Deformation and flutter speed

The simplified procedure for the calculation of the linear and nonlinear displacements and the flutter speed estimation is presented in Figure 4-2.

After extracting the necessary data from the provided model, a MDOGUI model was built. Subsequently, the structural deflections, linear and nonlinear, for different flight conditions were calculated and compared. In Figure 4-3 the displacements relative to the half wing span are presented: in a) the displacement is shown for varying angles of attack at a constant altitude (sea level); and the graph b) shows the displacement for different altitudes, related here with dynamic pressure, at a constant angle of attack (5°). As one can notice, the maximum displacements are around 15% (see Figure 4-3b). However, the deformations differ more for increasing displacement, whereas the distinction is still relatively low. This coincides with the literature, where the nonlinear effects reportedly show stronger effects upward 20%. A further explanation is given in the thesis [8].

For the flutter speed, the models were analysed with Nastran. It should be noted, that the structural damping is set to zero.

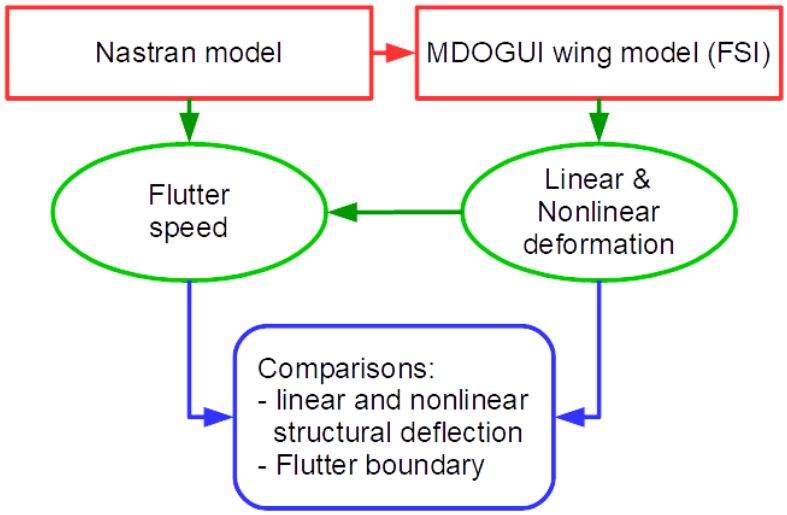

Figure 4-2: Work flow for the deformations and the flutter speed

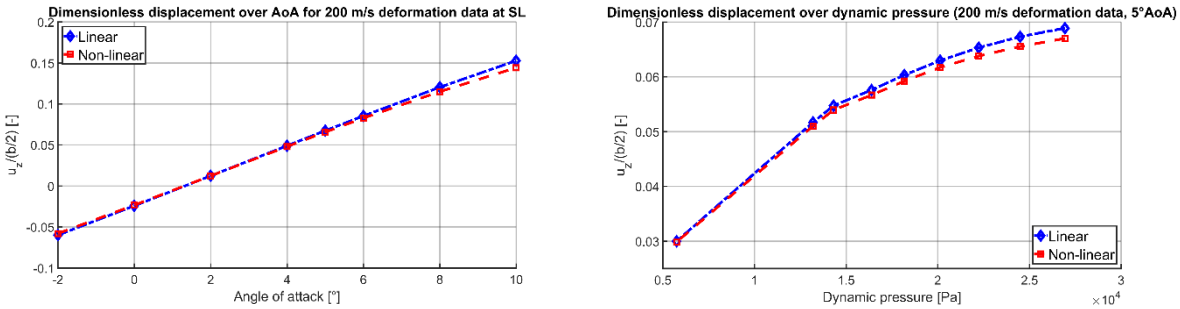

a) Dimensionless displacement for angles of attack between -2° and 10°

b) Dimensionless displacement for altitudes ranging from -1000m to 12497m

Figure 4-3: Displacement comparison for increasing angles of attack (a) and increasing altitude

In Figure 4-4, an example for a v-g (a) and a v-f graphs (b) for identifying the flutter phenomenon is given. For all cases, if flutter was observed, the corresponding modes were the first 4 modes. Whereas it was not ascertainable, which modes exactly couple, it could be assumed that the first bending mode and the first torsion mode couple (which is the most obvious interpretation from the graphs). Thus, a bending-torsion flutter is suspected to occur. To clarify which is the flutter mechanism happening,

experiments are necessary. The unstable chord mode was close to the damping border and even seemed to converge with increasing speed. Opposing, the torsional mode diverged, when the damping became positive. At around 320 m/s, for the first bending mode, a divergence appears, observable with the drop of the frequency to zero.

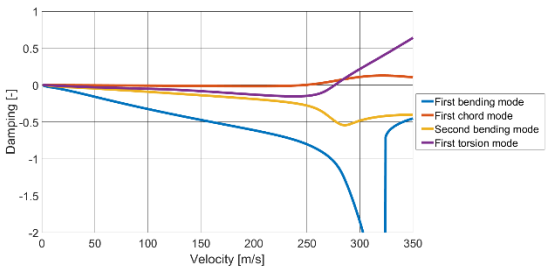

a) v-g graph for the linear deformed wing at 200 m/s, 10° angle of attack and at sea level

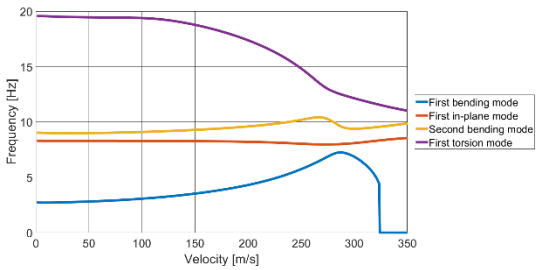

b) Corresponding v-f graph for the case in a)

Figure 4-4: Exemplary v-g and v-f graph

The flutter boundaries for a varying angle of attack and a variation in altitude are shown in Figure 4-5. For each wing, the appearing flutter speeds within the examination range (0 m/s to 350 m/s), were separated for the in-plane mode and the torsion mode. Regarding the angles of attack, the most obvious difference between the rigid and the deformed wing is the flutter mode behaviour. For small angles of attack, the rigid wing starts fluttering within the in-plane mode, while for the deformed wings it is the torsion mode (see Figure 4-5 a)). This changes for higher angles of attack, where the critical flutter mode of the rigid wing is the torsional mode and for the deformed wings it is the chord mode. Furthermore, the slope of the flutter boundary for the rigid and deformed wings have converse behaviour. The difference in the flutter speed appearance regarding the torsional mode can be explained by the downwash twist of the wing and the resulting twist for the deformed wing, opposing the flutter trend. For the flutter speeds regarding the altitude, the trend is almost linear, increasing flutter speed with increasing altitude (see Figure 4-5 b)). Above 6000m, no flutter was observable. Also, results above the speed of sound should be taken with care, as the DLM is only valid in subsonic regime. The rigid wing starts fluttering always after the deformed one, with the torsional mode compared to the chord mode.

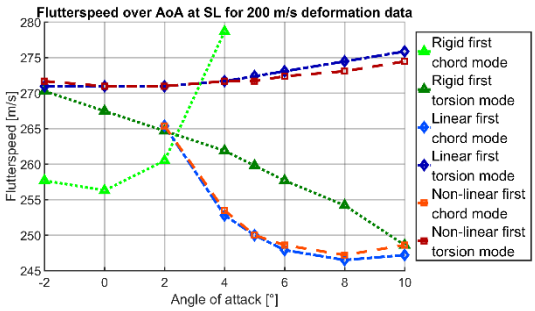

a) Flutter speeds vs angle of attack

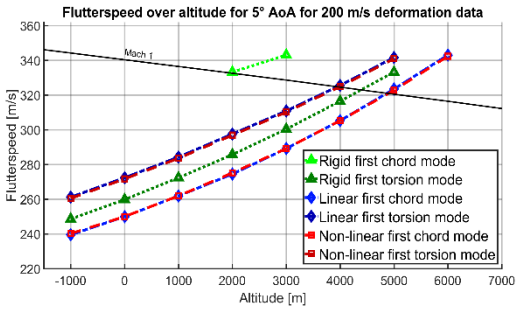

b) Flutter speeds vs altitude

Figure 4-5: presentation of the flutter speeds

4.3. Parametric study

A parametric study was carried out to investigate the feasibility of a mass reduction. First, the thickness parameter of the wing box was selected. Reducing it, not only reduces the mass but also changes the geometric properties. For several cases, new flutter analyses were done to evaluate the effect of a 10% and 20% thickness reduction. The resulting displacements were higher, up to 10% and 25%, respectively. The flutter boundary, behaving in a similar way, lowered by 5% and 10%, respectively, which corresponds to a lowering of 13m/s and 25m/s. A short overview of the results is given in Table 4-1 and Table 4-2. Thus, for a wing mass reduction of 7.3%, the flutter speed decreases almost 5%. With a mass saving of 14.6%, the flutter boundary was lowered between 6% and 11%, depending on the flutter mode.

Angle of attack [°]	z_t [m]	$z_{0.9t}$ [m]	|Δ| [%]	$z_{0.8t}$ [m]	|Δ| [%]
2°, linear deformed	0,159	0,143	10.06	0,117	26.42
2°, nonlinear deformed	0.159	0.143	10.06	0.119	25.16
10°, linear deformed	1,984	2,071	4.39	2.164	9.07
10°, nonlinear deformed	1.872	1.944	3.85	2.017	7.75

Table 4-1: Parametric study results for the wing tip displacement

Angle of attack [°]	$v_{Fl,t}$ [m]	$v_{Fl,0.9t}$ [m]	|Δ| [%]	$v_{Fl,0.8t}$ [m]	|Δ| [%]
2°, linear deformed, in-plane mode	265.37	256.28	3.43	248.59	6.32
10°, linear deformed, in-plane mode	247.19	235.30	4.81	219.21	11.32
2°, nonlinear deformed, in-plane mode	265.37	256.28	3.43	248.59	6.32
10°, nonlinear deformed, in-plane mode	248.59	236.70	4.78	224.11	9.85
2°, linear deformed, torsion mode	270.97	258.38	4.65	244.39	9.81
10°, linear deformed, torsion mode	275.86	263.27	4.56	249.99	9.38
2°, nonlinear deformed, torsion mode	270.97	258.38	4.65	244.39	9.81
10°, nonlinear deformed, torsion mode	274.46	262.58	4.33	249.29	9.17

Table 4-2: Parametric study results for the flutter speeds regarding the in-plane and the torsional modes

4.4. Static stability derivatives

To characterize the stability of the wing, a static stability derivative, namely C_{m_α}, was estimated for the rigid and the deformed wing. For this analysis the procedure adopted is presented in Figure 4-6.

For the CFD simulations in ANSYS CFX, the wing shapes were first calculated with the MDOGUI tool and with the result data a CAD model was built as intermediate step. With a surrounding block, a fluid space was modelled that could then be used for the CFD simulations. In connection a comparison between the wing models took place. It should be mentioned that the results for the rigid wing at 10° angle of attack did not reach a steady solution. The occurring oscillation is suspected to be caused by insufficient mesh resolution.

For the coefficients of lift, moment and drag (C_L, C_m, C_D, respectively) the curves are shown in Figure 4-7 a) - c). One can recognize that the difference between the results of the linear and nonlinear deformed shapes is not much. As stated before, the displacement difference for those cases is also small. Thus, no remarkable difference was expected. It is also noticeable that with the deformation the slope for both the lift and moment coefficient is lower. This seems appropriate, as with the deformation, the effective wing span is shortened as well as with a twist, the effective angle of attack along the wing span is reduced. While the curve of drag has a shallower slope for the deformed wings, the ratio C_D/C_L has a steeper trend (see Figure 4-7 d)).

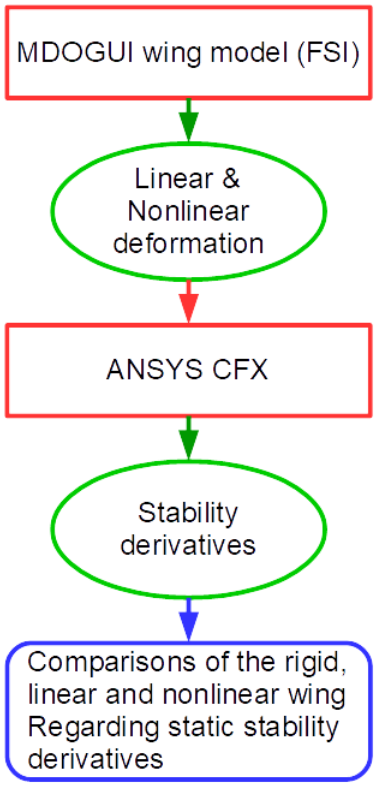

Figure 4-6: Workflow derivatives

In Figure 4-1, the trend of the static stability derivative, C_{m_α}, is presented. It is noticeable that the rigid wing is in a more stable range than the deformed ones. Nevertheless, all three have a stable behaviour. With increasing angles of attack, the gradient of the curves becomes more positive, indicating a possible instability coming up with further increasing angles. In sum, the wing can be assumed as statically stable in the examined range, eligible for the rigid wing as well as for the deformed ones.

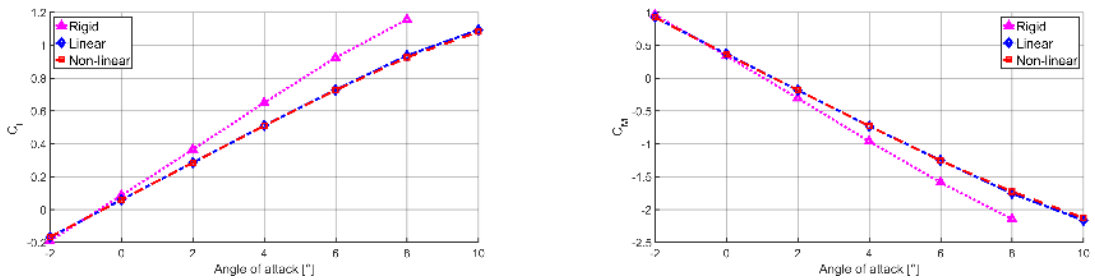

a) Lift coefficient

b) Moment coefficient

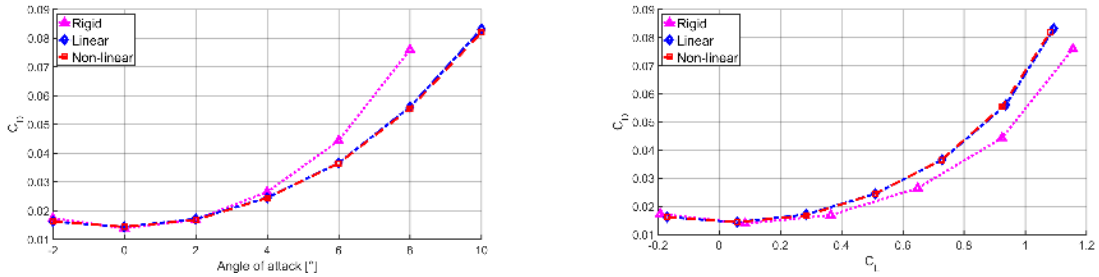

c) Drag coefficient

d) Drag over Lift coefficient

Figure 4-7: The coefficients of a) lift, b) moment, c) drag and d) drag over lift coefficient

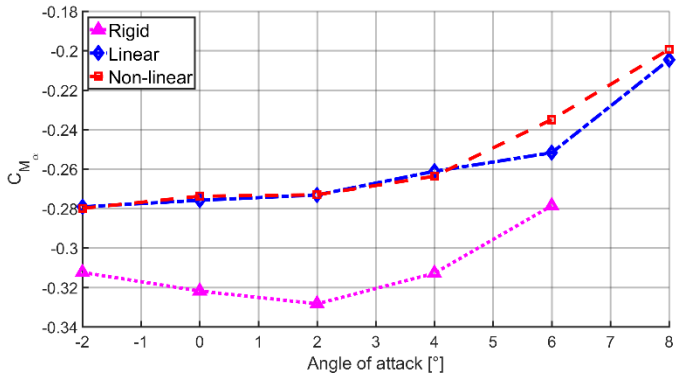

Figure 4-1: trend of C_{m_α} for the rigid wing and deformed wings

5. Conclusion and future work

The main goal of this thesis was to investigate the influence of linear and nonlinear structural deflection on the performance of a given high aspect ratio wing. For this purpose, the displacements, linear and nonlinear, were calculated in MDOGUI. Perceptible differences between the linear and nonlinear deformations could not be noticed. However, a trend was recognized, as the wing experiences larger deformations the difference between linear and nonlinear displacements increase. Following, the flutter speeds for the deformed wing as well as for the rigid wing were estimated and compared. They also did not differ extraordinarily between the two deformed shapes, whereas a comparison to the rigid wing showed noticeable variations. For the static stability derivative, a difference between the rigid and the deformed wing was determined, while the stability behaviour itself was not influenced in a strong way.

There are still several open points that could not be addressed in this work. To characterize the stability behaviour of the wing, rigid and deformed, an estimation of the dynamic stability derivatives should be done. Further, the calculation of the deformation was performed within a lower subsonic range than the aircraft is intended to operate. Thus, determination within the transonic regime should be considered. For this purpose, the MDOGUI must be adapted, as it cannot examine aerodynamic nonlinearities (such as shock and boundary separation) yet. With a higher velocity, larger displacements are expected, leading to more distinct differences between the linear and nonlinear structural deflections.

6. References

[1] F. Afonso, J. Vale, É. Oliveira, F. Lau and A. Suleman, "A review on non-linear aeroelasticity of high aspect-ratio wings," *Progress in Aerospace Sciences,* 2017.

[2] R. L. Bisplinghoff, H. Ashley und R. L. Halfman, Aeroelasticity, Mineola, New York: Dover Publications, Inc., 1955.

[3] D. A. Babcock, *Aircraft Stability Derivative Estimation from Finite Element Analysis, Master thesis,* 2002.

[4] A. C. Limache, *Aerodynamic Modeling Using Computational Fluid Dynamics and Sensitivity Equations, Dissertation,* Blacksburg, Virginia, 2000.

[5] B.-g. Mi, H. Zhan and B.-b. Chen, "New Systematic CFD Methods to Calculate Static and Single Dynamic Stability Derivatives of Aircraft," *Mathematical Problems in Engineering,* Volume 2017, 11 pages, 2017.

[6] C. A. Mader and J. R. R. A. Martins, "Computing Stability Derivatives and Their Gradients for Aerodynamic Shape Optimization," *AIAA Journal, Vol. 52, No. 11,* pp. 2533-2546, November 2014.

[7] F. Afonso, G. Leal, J. Vale, É. Oliveira, F. Lau and A. Suleman, "The effect of stiffness and geometric parameters on the nonlinear aeroelastic performance of high aspect ratio wings," *Proceedings of the Institution of Mechanical Engineers, Part G: Journal of Aerospace Engineering,Vol 231, Issue 10,* pp. 1824 - 1850, 2017.

[8] M. Sohst, *Effects of linear and nonlinear structural deflections on the performance and stability derivatives of high-aspect ratio wing aircraft,* 2017.